Key Engineering Materials
ISSN: 1662-9795, Vol. 926, pp 1581-1590
doi:10.4028/p-7t1lyj

Submitted: 2021-11-26
Revised: 2022-01-21
Accepted: 2022-02-02
Online: 2022-07-22

Influence of the Workpiece Material and Cooling Condition on the Texture Obtained through Ultrasonic Vibration-Assisted Machining

R. Bertolini[1,a*], I. Castagnotto[1,b], A. Ghiotti[1,c] and S. Bruschi[1,d]

[1]University of Padova, Department of Industrial Engineering, via Venezia 1, 35131, Padova, Italy

[a*]rachele.bertolini@unipd.it, [b]ilaria.castagnotto@studenti.unipd.it, [c]andrea.ghiotti@unipd.it, [d]stefania.bruschi@unipd.it

Keywords: Ultrasonic vibration-assisted machining, Hybrid machining, Cryogenic cooling, Texture.

Abstract. Ultrasonic Vibration-Assisted Machining (UVAM) has been investigated as one of the most suitable methods to imprint patterns on metal surfaces. Actually, UVAM, as a consequence of the superimposition of a high-frequency and small-amplitude vibration to the cutting tool motion, makes possible the generation of micro-textured surfaces. On the basis of the vibration pattern and parameters, cutting process and tool characteristics, micro-dimples of different morphology and dimension can be obtained. However, the literature review has evidenced that none of the available studies considered the influence of the cooling conditions as well as the workpiece material on the obtainable dimples geometry. To this aim an UVAM experimental campaign was carried out at varying cutting speed, workpiece material and cooling conditions. Then, the surface finish was evaluated in terms of dimples size and surface roughness. Experimental results showed that deeper dimples are obtained for materials characterized by higher elastic modulus and machined under cryogenic cooling.

Introduction

Ultrasonic Vibration-Assisted Machining (UVAM) has been investigated as one of the most suitable methods to conferee patterns on material surfaces, such as metals. It represents a non-traditional machining method that exploits a transducer to convert high-frequency electrical energy into mechanical vibration energy to be applied to the cutting tool during machining. As a consequence, the cutting process results into the generation of micro-textured surfaces [1], characterized by the so called "*dimples*". Such unique textures can be exploited for different purposes. In [2], textured surfaces produced by UVAM were shown to have superior tribological properties in terms of average friction coefficient, wear rate and adhesion compared to conventionally machined ones. Ultrasonic Vibration-Assisted Turning (UVAT) was also proved as a suitable approach to increase wettability of the AA7075-T6 aluminum alloy in [3]: regardless of the adopted process parameters, wettability was improved thanks to the application of ultrasonic vibration to the tool, further increased by the vibration modes. In [4], the wettability enhancement provided by UVAT was exploited to increase the deposition performances of a sol-gel coating on a magnesium alloy.

Therefore, the knowledge about the effect of process parameters on the dimples shape is essential to tune the surface-dependent properties. Nevertheless, there are only few systematic studies dealing with the fabrication of microtextured surfaces through UVAM. In [5], the versatility of UVAT was demonstrated by cutting outer, face and inner surfaces of different materials. In [6], the effect of different parameters, like the tool radius, tool clearance angle and tool wear, on the generated surface texture was studied. The clearance angle was shown to have a strong impact on the dimples profiles along the cutting direction, whereas sharper tool radii produced tighter dimples. It was also demonstrated that tool materials harder than carbides were generally to be preferred since they contributed to the formation of well-shaped and more homogeneously distributed dimples.

Also cryogenic cooling has emerging in machining of metal alloys, being capable to enhance the machined parts functional performances. As a matter of fact, dry machining suffers from too high heat generation, which, in turn, increases tool wear and decrease the machined surface integrity. It is worth noting that, under dry cutting conditions, heat generation is further exasperated in case of

UVAM, as recently pointed out in [4]. To this reason, cryogenic cooling can be coupled to UVAM to generate peculiar textures, having a potential appeal for wettability enhancement or wear reduction.

On the light of the above reported literature review, the present study aims at evaluating the effect of the workpiece material and cooling condition on the dimples geometrical characteristics produced by UVAM. To this aim, a UVAT experimental campaign was carried out at varying cutting speed, namely 100 m/min and 200 m/min, under dry and cryogenic cooling conditions and applied to different metals (magnesium alloy, titanium alloy, and stainless steel). Afterwards, the surface finish of textured samples was assessed by optical profiler. Finally, the state of the cutting tool after machining was analyzed by means of scanning electron microscopy.

Theoretical model. The geometrical characteristics of the dimples generated through UVAT were modelled on the basis of the cutting path represented by a sinusoid that is function of time (t), as shown in Fig. 1 [7,8].

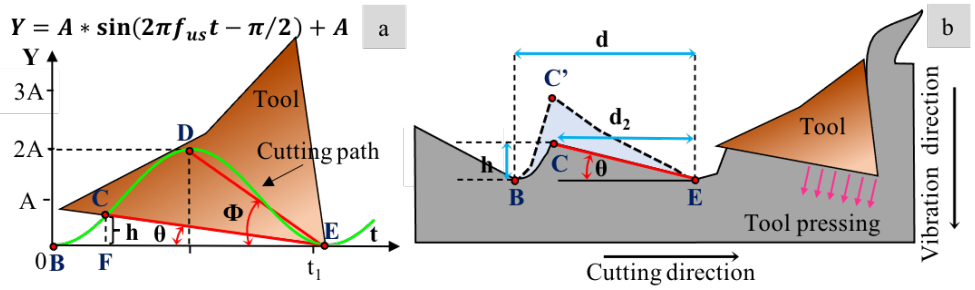

Fig. 1. *Theoretical cutting path as a function of time (a), comparison between theoretical and displaced profile of a dimple along the cutting direction (b).*

The distance (d) between two adjacent dimples along the direction of cut, i.e. the width of dimples given by the distance BE (Fig. 1b), can be calculated through the following Eq. 1:

$$d = \frac{V}{f_{us}} \tag{1}$$

where f_{us} is the ultrasonic vibration frequency (Hz). When the tool reaches point E (Fig. 1a), its flank face intercepts the cutting path at point C, identifying an angle of intersection (θ), which is approximately equal to the clearance angle of the tool (β). An intersection ratio (σ) is proposed to determine the intersection between the tool path and its flank face given by Eq. 2:

$$\sigma = \tan\phi = \frac{4A}{d} \tag{2}$$

The distance d_2 is the distance between the projection of the point C along cutting direction and the point E given by the distance FE (Fig 1b); it is given by Eq. 3:

$$d_2 = \frac{d}{1+\frac{\tan\theta}{\tan\phi}} \tag{3}$$

Given the cutting conditions of the present study, the tool flank always intercepts the cutting trajectory being $\sigma > \tan(\beta)$; considering the triangle similarity criteria, the length of CF in Fig. 1a, i.e. the depth of dimples in cutting direction (h), can be calculated from Eq. 4:

$$h = d_2 \tan\theta \tag{4}$$

By using the proposed model, the geometrical characteristic of the dimples can be unambiguously calculated.

Experimental

Materials.

The aim of the present study is to evaluate the effect of the workpiece material and cooling conditions on the dimples geometrical characteristics produced by UVAM. To pursue this goal, three

different workpiece materials, namely AZ31 magnesium alloy, grade 2 titanium alloy and AISI 316L stainless steel, were chosen in virtue of their different elastic modulus.

Table 1 *Mechanical properties of the investigated materials [9,10,11].*

Material	Elastic modulus (GPa)	Poisson's coefficient (-)	Hardness (HV)
AZ31	45	0.35	65
Ti (grade-2)	108	0.35	171
AISI 316L	193	0.31	284

Machining tests – surfaces texture generation.

Two surface texturing processes, namely Ultrasonic Vibration-Assisted Machining (UVAM) and Cryogenic Ultrasonic Vibration-Assisted Machining (CUVAM), were carried out on a Mori Seiki™ NL 2500 CNC lathe.

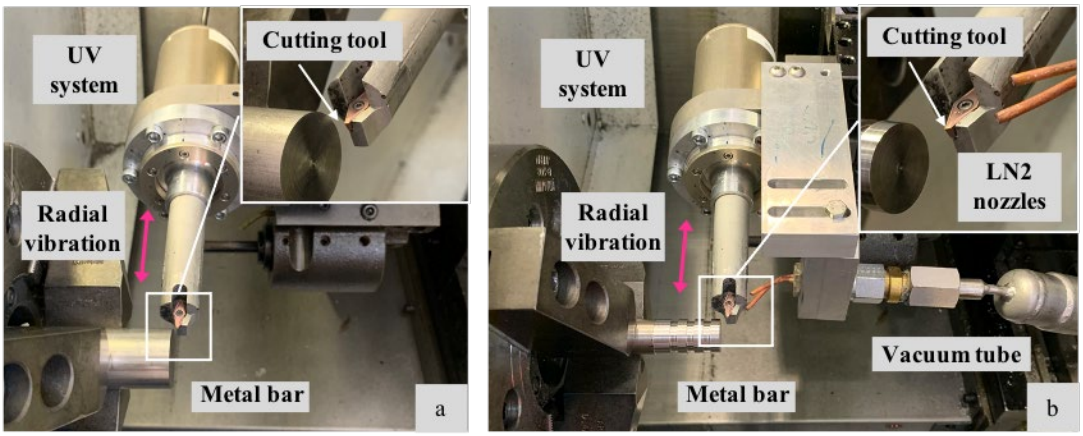

Fig. 2 *UVAM setup (a) and CUVAM setup (b) with zoom details.*

Fig. 2a shows the UVAM setup, which consists of an Ultrasonic Vibration (UV) system mechanically fixed at the tool turret, and a generator that is placed externally. Details about the UVAM experimental setup can be found in [12].

To perform CUVAM, the UVAM setup was equipped with a cryogenic cooling sub-system. The latter includes a dewar, in which liquid nitrogen (LN2) is stored, a vacuum jacketed hose to carry LN2, and two copper nozzles with 0.9 mm diameter that were used to spray LN2 towards the tool flank and rake faces. Details about the cryogenic cooling sub-system can be found in [8].

During UVAM e CUVAM, the cutting tool vibrates along the radial direction at a frequency (f_{us}) of 30 kHz and amplitude (A) of 5 μm. A VCEX 110301L-F 1125 insert, suitable to machine both heat-resistant and light-weight alloys, was chosen as cutting tool. It is characterized by a rake angle (α) of 5° 30', clearance angle (β) of 7° and nose radius (R) of 0.1 mm. The feed (f) and depth of cut (DoC) were kept fixed to 0.05 mm/rev and 0.05 mm, respectively.

Two cutting speed (V), namely 100 m/min and 200 m/min, were adopted to investigate their effect on the dimples shape.

Surface texture characterization. The machined surface topography was evaluated using the Sensofar™ Plu-Neox optical profiler by means of 20X Nikon™ confocal objective. Fig. 3 shows the experimental equipment with a zoom of the workpiece under characterization clamped on a jaw.

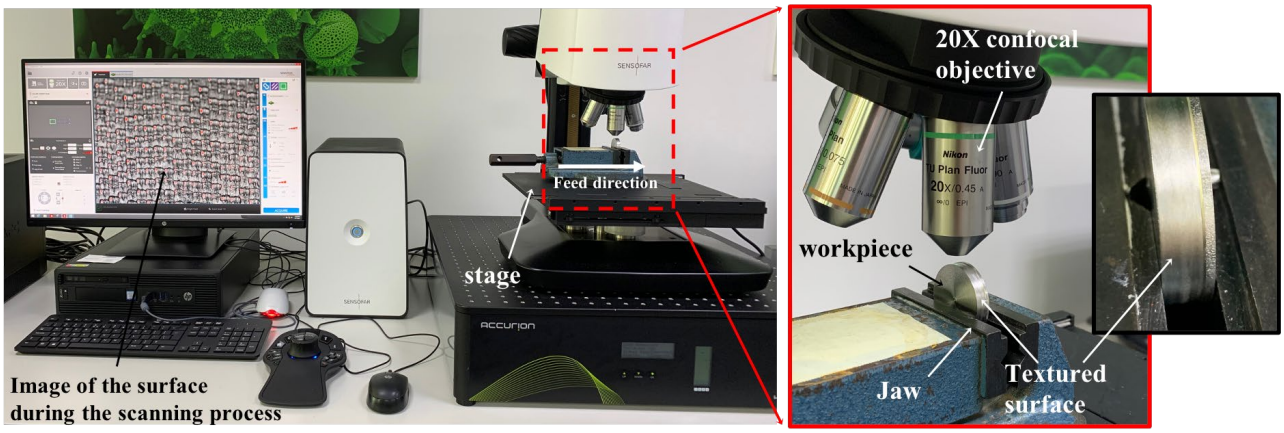

Fig. 3 *Sensofar^{TM} Plu-Neox optical profiler used to characterize the surface finish generated by UVAM and CUVAM.*

Areal and profile surface roughness parameters according to ISO 25178-2:2012 and ISO 4287:2009, respectively, were computed after outliers and form removal using Gaussian filtering according to ISO 16610-61:2011. For each sample, 3 sections were scanned and the roughness evaluated. Afterwards, for each measurement, 10 roughness profiles were extracted to compute measurements on the dimples shape.

To fully characterized the surface topography generated by UVAM and CUVAM, the following surface roughness parameters were taken into consideration:

- the average surface roughness (Sa), for general reference, since it is the most commonly used indicator for surfaces comparison;
- the mean width of the profile elements (RSm), which can be taken as indicator of the dimples width (d) [7];
- the maximum height of profile (Rz*),* which can be taken as indicator of the dimples depth (h) [7];

Besides the aforementioned parameters, the distance between the peak projection along the cut direction (d_2) was calculated (see Fig.1).

Tool wear characterization. To consider the effect of the tool wear on the surface finish, each cutting tool was inspected after UVAM and CUVAM. The FEI QUANTA 450™ Scanning Electron Microscope (SEM) equipped with the Everhart Thornley Detector (ETD) and Backscattered Electron Detector (BSED) was used to acquire images of the tools and, therefore, identify the tool wear mechanisms. Specifically, the tool rake and flank faces were observed at 200X and 500X magnifications. Fig. 4 shows the SEM experimental equipment with zoom of the tool placed on the holder of the vacuum chamber.

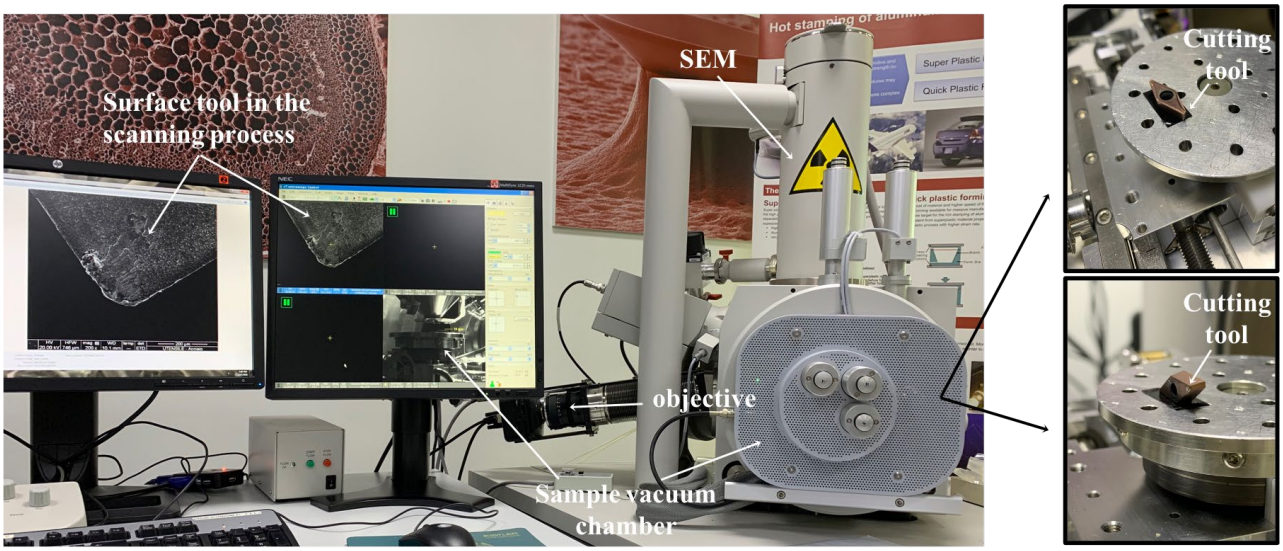

Fig. 4 *FEI QUANTA 450™ SEM setup during cutting tool image acquisition with different views of the tool placed inside the vacuum chamber.*

Results and Discussion

Elastic recovery analysis. Example of UVAM and CUVAM surface textures with typical surface roughness profiles obtained in case of Vc=100 m/min and d=0.05 mm is shown in Fig. 5 for different workpiece materials.

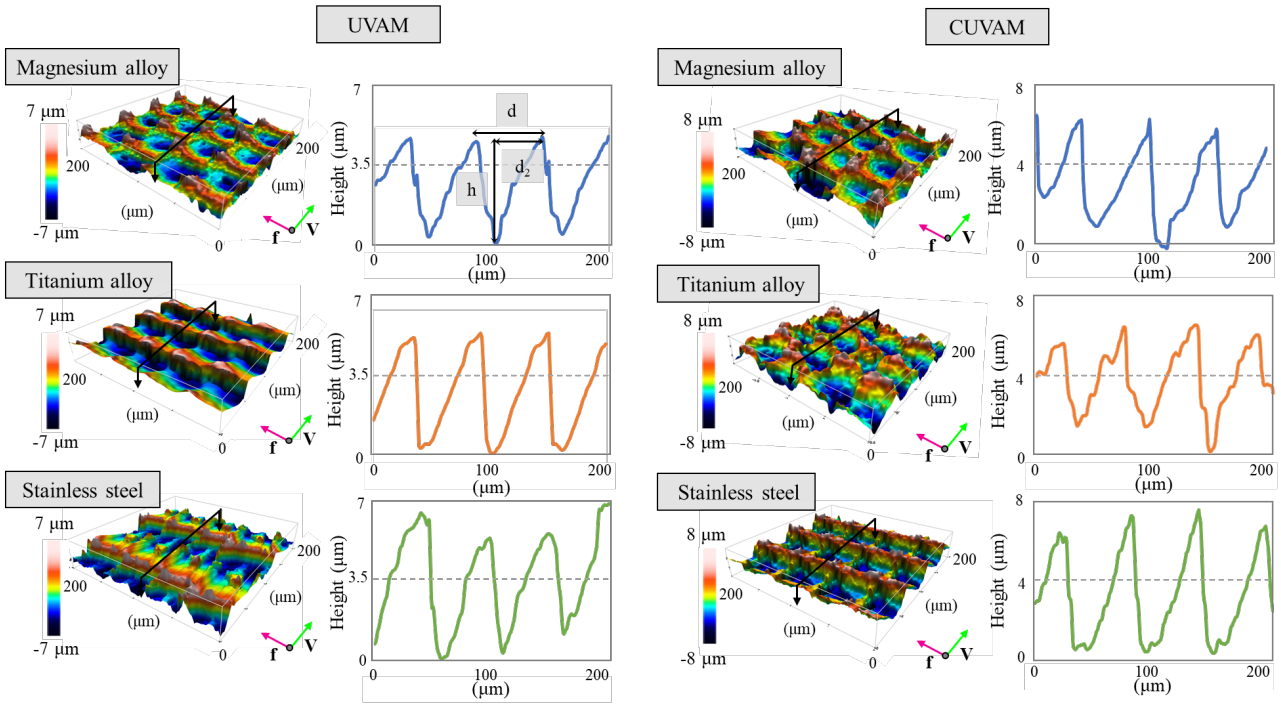

Fig. 5 *Example of textures obtained after UVAM and CUVAM with Vc = 100 m/min at varying workpiece material.*

Both UVAM and CUVAM allowed the generation of geometrically-defined dimples, indicating that surface texturing is possible even in the case of cryogenic environment and regardless of the investigated workpieces material.

Table 2 reports the theoretical values of *d*, d_2 and *h* calculated according to the model previously described, whereas in table 3 the experimental measured values are summarized.

Fig. 6 graphs the experimental dimple depth values as a function of the cutting speed, cooling condition and workpiece material. From the graph, it is possible to say that the higher the elastic

modulus the higher the dimples depth. For example, under UVAM at Vc=100 m/min and d=0.05 mm, the dimples depth increases of 29% and 37% for titanium alloy and stainless steel compared to magnesium alloy, respectively. This can be ascribed to the fact that the material undergoes an elastic recovery after the tool disengagement that is greater on the textured surface peaks generated on the stainless steel due compared to that on the magnesium alloy due to the differences in their elastic modulus. As a consequence of that, the material in correspondence of the dimple peak shifts from point C to point C' (see Fig. 1 for reference).

Similarly, the displacement along the cutting direction is greater in the case of CUVAM than in the case of UVAM, due to the increased strain hardening induced by the lower cutting temperatures induced by the cryogenic cooling. For this reason, CUVAM allows the formation of deeper dimples than UVAM [8]. Differences among UVAM and CUVAM are mitigated at the highest cutting speed, since higher strain rates contribute to increase the material elastic restoration.

From the above analysis it emerges the limit of the theoretical model for an accurate prediction of the dimples depth, since this model neglects the mechanical characteristics of the material under deformation [7].

Fig. 7 graphs the experimental dimple width values as a function of the cutting speed, cooling condition and workpiece material. A similar trend is obtained for d_2, therefore the graph is here omitted. It can be said that a rather accurate estimation of the experimental values was provided by the theoretical model for both d and d_2 being the error range within the 8% and 15% respectively, thus witnessing the accuracy of the model in predicting the dimple width, as highlighted from the comparison of the experimental values with those listed in Table 2.

Table 2 *Theoretical values of the dimples depth (h) and distances (d, d_2) for the investigated workpieces materials.*

Cutting speed (m/min)	Width d (µm)	Distance d_2 (µm)	Depth h (µm)
100	55.56	41.42	5.06
200	111.11	66.05	8.07

Table 3 *Experimental values of the dimples depth (h) and distances (d, d_2) for the investigated workpieces materials after UVAM and CUVAM.*

Machining strategy	Cutting speed (m/min)	Width (d) (µm)	Distance (d_2) (µm)	Depth (h) (µm)
Magnesium alloy				
UVAM	100	55.52 ± 1.27	36.01 ± 1.66	3.89 ± 0.25
	200	120.94 ± 6.77	77.88 ± 7.76	8.77 ± 0.56
CUVAM	100	56.30 ± 0.9	41.49 ± 0.73	6.2 ± 0.9
	200	114.38 ± 3.55	72.80 ± 0.98	9.6 ± 0.42
Titanium alloy				
UVAM	100	56.67 ± 0.78	47.78 ± 2.07	5.50 ± 0.18
	200	115.73 ± 1.82	72.20 ± 2.59	9.13 ± 0.37
CUVAM	100	57.00 ± 1.04	41.34 ± 0.94	7.22 ± 0.57
	200	116.22 ± 3.83	72.55 ± 4.2	9.82 ± 0.55
Stainless Steel				
UVAM	100	55.79 ± 0.72	39.67 ± 2.19	6.21 ± 0.4
	200	111.20 ± 1.43	74.11 ± 3.74	9.87 ± 0.55
CUVAM	100	56.70 ± 0.83	41.38 ± 0.93	7.38 ± 0.2
	200	110.41 ± 0.83	77.43 ± 1.33	10.17 ± 0.75

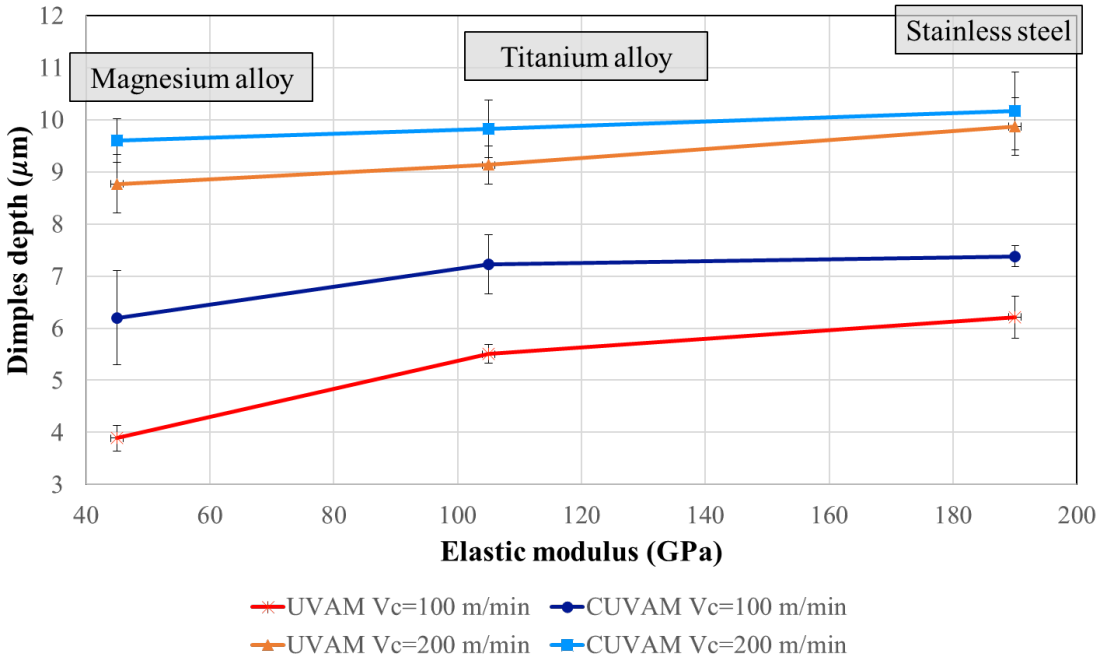

Fig. 6 *Dimples depth as a function of the cutting speed, cooling condition and workpiece material.*

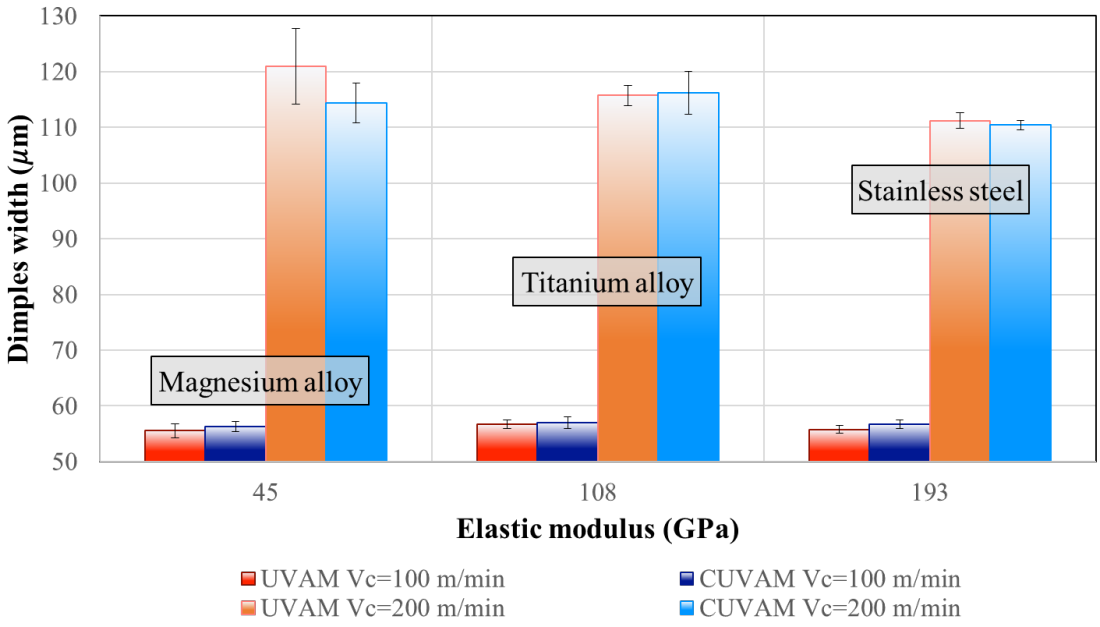

Fig. 7 *Dimples width as a function of the cutting speed, cooling condition and workpiece material.*

Surface roughness analysis. Table 4 shows the average surface roughness Sa of the surfaces generated by UVAM and CUVAM at varying workpiece material, cutting speed and cooling condition. In general, rougher surfaces were generated by CUVAM compared to UVAM. Compared to UVAM, at the lowest cutting speed, CUVAM increases the surface roughness of 45%, 11% and 23% for the magnesium alloy, titanium alloy and stainless steel, respectively. This can be attributed to the dimples expansion along the vibration direction. Similarly, the highest surface roughness is obtained at the highest cutting speed due to the dimples depth increase.

Table 4 *Surface roughness as a function of the cutting speed, cooling condition and workpiece material.*

Machining strategy	Material	Vc = 100 m/min	Vc = 200 m/min
UVAM	Magnesium alloy	0.87 ± 0.07	1.98 ± 0.19
	Titanium alloy	1.53 ± 0.03	1.60 ± 0.08
	Stainless steel	1.32 ± 0.17	2.09 ± 0.25
CUVAM	Magnesium alloy	1.59 ± 0.1	2.49 ± 0.26
	Titanium alloy	1.38 ± 0.12	1.94 ± 0.29
	Stainless steel	1.71 ± 0.15	2.02 ± 0.31

Tool wear. Fig. 8 and Fig. 9 show the wear of the tool flank and rake faces after UVAM and CUVAM, respectively. It is worth noting that solely images of the tool after machining the titanium alloy and stainless steel were reported, being the tool wear after machining the magnesium alloy negligible.

Firstly, it can be easily seen that more pronounced wear characterized the cutting tools that machined the stainless steel. This can be ascribed to the highest mechanical properties that characterized the stainless steel compared to the other two workpiece material under investigation (see Table 1). Secondly, wear of the cutting tool was limited when CUVAM was adopted instead of UVAM. In fact, the abduction of liquid nitrogen during machining contributes to reduce the temperature in the cutting zone, and, consequently, to maintain the tool hardness. This is in accordance to previous literature studies dealing with the tool wear under dry and cryogenic cutting conditions [13].

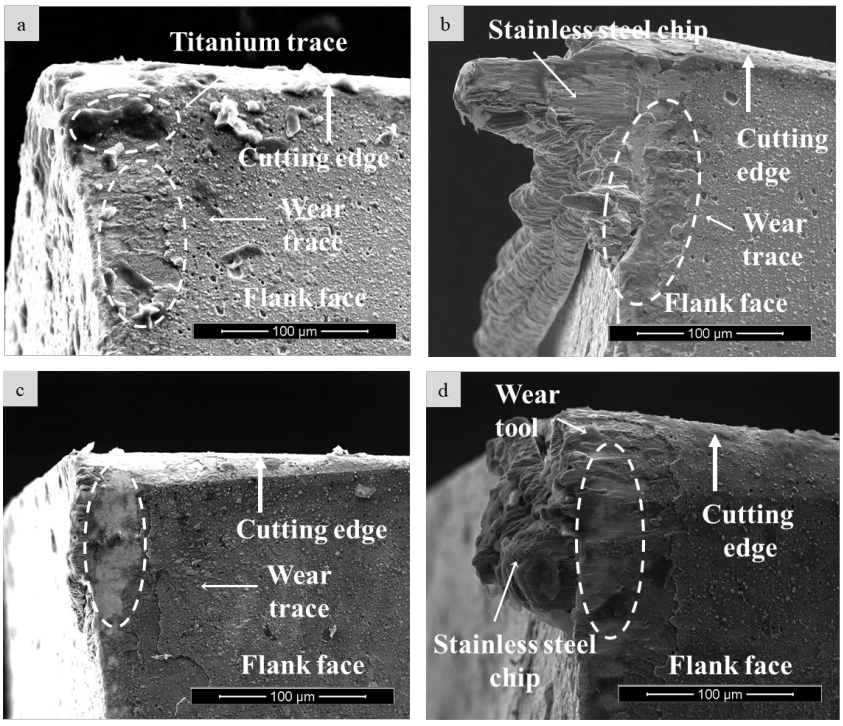

Fig. 8 *SEM images of the tool flank face after machining: (a) titanium alloy, UVAM, (b) stainless steel, UVAM, (d) titanium alloy, CUVAM, (e) stainless steel, CUVAM.*

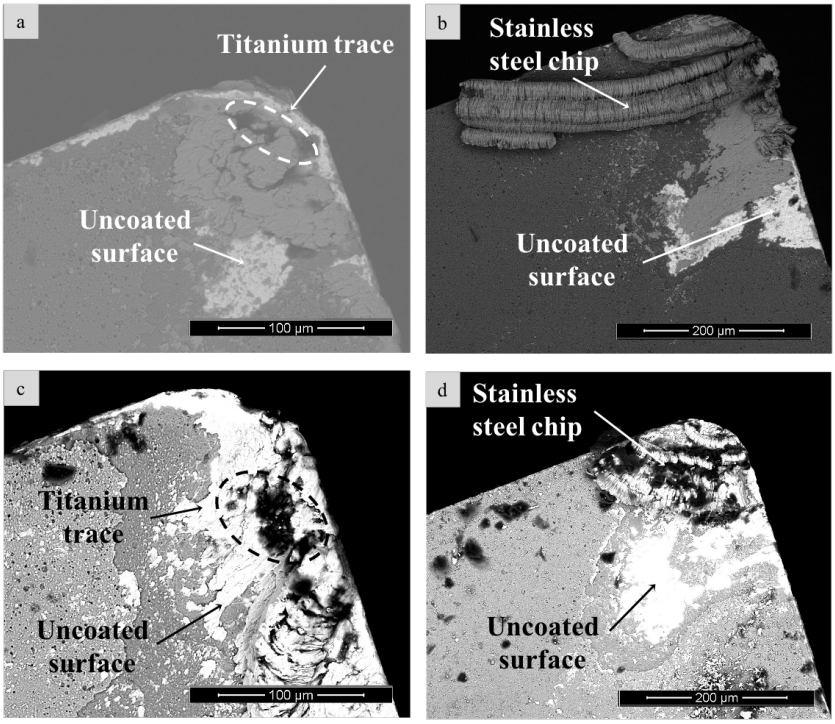

Fig. 9 *SEM images of the tool rake face after machining: (a) titanium alloy, UVAM, (b) stainless steel, UVAM, (d) titanium alloy, CUVAM, (e) stainless steel, CUVAM.*

Conclusions

The present study investigates the influence of the workpiece material and cooling condition on the texture obtained through ultrasonic vibration-assisted machining. To this aim, UVAM and CUVAM turning experimental campaigns were performed on three different materials, namely a magnesium alloy, a titanium alloy, and a stainless steel at varying cutting speed. Afterwards, the textured surfaces were characterized and the tool wear evaluated.
The main findings can be summarized as follows:

- Deeper dimples are generated at increasing workpiece material elastic modulus. This can be attributed to the fact that the material experiences higher elastic recovery after the tool disengagement.
- Similarly, wider dimples are generated in the case of CUVAM, due to the higher strain hardening induced by the lower temperatures that characterize cryogenic cooling that occur during the former process rather than in the latter. Nevertheless, at increasing cutting speed, the differences between UVAM and CUVAM are mitigated by the rise of the cutting temperature.
- Neglecting the elastic recovery represents the main source of inaccuracy of the theoretical model that describes the dimples geometrical characteristics.
- In general, rougher surfaces in terms of Sa were generated using CUVAM compared to UVAM due to the presence of deeper dimples along the cutting direction for the reasons explained above. The same effect was obtained at the highest cutting speed.
- The cutting tools that machined the stainless steel were characterized by the highest wear; nevertheless, CUVAM helped in reducing the tool wear thanks to the containment of the temperature rise.

Acknowledgments

This research was carried out in the framework of the project PRIN 201742RB8R_002 “Bionic” funded by the Italian Ministry of University and Research.

References

[1] T. Koyano, A. Hosokawa, T. Takahashi, T. Ueda, One-process surface texturing of a large area by electrochemical machining with short voltage pulses, CIRP Annals 68(1) (2019) 181-184.

[2] S. Amini, H.N. Hosseinabadi, S.A. Sajjady, Experimental study on effect of micro textured surfaces generated by ultrasonic vibration assisted face turning on friction and wear performance, Appl. Surf. Sci. 390 (2016) 633-648.

[3] H.N. Hosseinabadi, S.A. Sajjady, S. Amini, Creating micro textured surfaces for the improvement of surface wettability through ultrasonic vibration assisted turning, Int. J Adv. Manuf. Technol. 96 (2018).

[4] R. Bertolini, S. Bruschi, A. Ghiotti, L. Pezzato, Ultrasonic Vibration Turning to Increase the Deposition Efficiency of a silica-based Sol-Gel Coating, Procedia Manuf. 34 (2019) 101-109.

[5] X. Liu, D. Wu, J. Zhang, X. Hu, P. Cui, Analysis of surface texturing in radial ultrasonic vibration-assisted turning, J Mater Process Technol. 267 (2019) 186-195.

[6] S. Amini, H.N. Hosseinabadi, S.A. Sajjady, Experimental study on effect of micro textured surfaces generated by ultrasonic vibration assisted face turning on friction and wear performance, Appl. Surf. Sci. 390 (2016) 633-648.

[7] X. Liu, J. Zhang, X. Hu, W. Wu, Influence of tool material and geometry on micro-textured surface in radial ultrasonic vibration-assisted turning,Int J Mech. Sci. 152 (2019) 545-557.

[8] A. Ghiotti, R. Bertolini, L. Pezzato, E. Savio, M. Terzini, S. Bruschi, Surface texturing to enhance sol-gel coating performances for biomedical applications, CIRP Annals. 70 (2021) 459-62.

[9] D. Gastaldi, V. Sassi, L. Petrini, M. Vedani, S. Trasatti, F. Migliavacca, Continuum damage model for bioresorbable magnesium alloy devices-Application to coronary stents, J. Mech. Behav Biomed Mater. 4(3) (2011) 352-365.

[10] C.N. Elias, D.J. Fernandes, F.M. de Souza, E. dos Santos Monteiro, R.S. de Biasi, Mechanical and clinical properties of titanium and titanium-based alloys (Ti G2, Ti G4 cold worked nanostructured and Ti G5) for biomedical applications, JMater Res Technol. 8(1) (2019) 1060-1069.

[11] I.O. Tugay, A. Hosseinzadeh, G.G. Yapici, Hardness and wear resistance of roller burnished 316L stainless steel, Mater Today: Proceedings. 47(2) (2021).

[12] E. Di Iorio, R. Bertolini, S. Bruschi, A. Ghiotti, Design and development of an ultrasonic vibration assisted turning system for machining bioabsorbable magnesium alloys, Procedia CIRP. 77 (2018) 324-327.

[13] A. Bordin, S. Bruschi, A. Ghiotti, P.F. Bariani, Analysis of tool wear in cryogenic machining of additive manufactured Ti6Al4V alloy, Wear. 328 (2015) 89-99.